Cross-Validation of a Glucose-Insulin-Glucagon Pharmacodynamics Model for Simulation using Data from Patients with Type 1 Diabetes

Wendt, Sabrina Lyngbye; Ranjan, Ajenthen; Møller, Jan Kloppenborg; Schmidt, Signe; Boye Knudsen, Carsten; Holst, Jens Juul; Madsbad, Sten; Madsbad, Sten; Madsen, Henrik; Nørgaard, Kirsten; Jørgensen, John Bagterp

Published in:
Journal of Diabetes Science and Technology

Link to article, DOI:
10.1177/1932296817693254

Publication date:
2017

Document Version
Peer reviewed version

Cross-Validation of a Glucose-Insulin-Glucagon Pharmacodynamics Model for Simulation using Data from Patients with Type 1 Diabetes

Sabrina Lyngbye Wendt, MScBME[1,2], Ajenthen Ranjan, MD[3,4], Jan Kloppenborg Møller, MSc, PhD[2], Signe Schmidt, MD, PhD[3,4], Carsten Boye Knudsen, MSc, PhD[1], Jens Juul Holst, MD, DMSc[5], Sten Madsbad, MD, DMSc[3,5], Henrik Madsen, MSc, PhD[2], Kirsten Nørgaard, MD, DMSc[3], John Bagterp Jørgensen, MSc, PhD[2]

Author affiliations: [1]Zealand Pharma, Glostrup, Denmark; [2]Department of Applied Mathematics and Computer Science, Technical University of Denmark, Kgs. Lyngby, Denmark; [3]Department of Endocrinology, Hvidovre University Hospital, Hvidovre, Denmark. [4]Danish Diabetes Academy, Odense, Denmark. [5]Faculty of Health and Medical Sciences, University of Copenhagen, Copenhagen, Denmark.

Sabrina Lyngbye Wendt
Zealand Pharma
Smedeland 36
DK-2600 Glostrup
Denmark
+45 88773643
slw@zealandpharma.com

Ajenthen Ranjan
Hvidovre University Hospital
Kettegård Allé 30
DK-2650 Hvidovre
Denmark
+45 38626378
ajenthen.ranjan.02@regionh.dk

Jan Kloppenborg Møller
Technical University of Denmark
Asmussens Allé, Building 303B
DK-2800 Kgs. Lyngby
Denmark
+45 45253418
jkmo@dtu.dk

Signe Schmidt
Hvidovre University Hospital
Kettegård Allé 30
DK-2650 Hvidovre
Denmark
+45 38622809
signe.schmidt@regionh.dk

Carsten Boye Knudsen
Zealand Pharma
Smedeland 36
DK-2600 Glostrup
Denmark
+45 88773614
cbk@zealandpharma.com

Jens Juul Holst
Panum Instituttet
Blegdamsvej 3
DK-2200 København N
Denmark
+45 35327518
jjholst@sund.ku.dk

Sten Madsbad
Hvidovre University Hospital
Kettegård Allé 30
DK-2650 Hvidovre
Denmark
+45 38623862
sten.madsbad@regionh.dk

Henrik Madsen
Technical University of Denmark
Asmussens Allé, Building 303B
DK-2800 Kgs. Lyngby
Denmark
+45 45253408
hmad@dtu.dk

Kirsten Nørgaard
Hvidovre University Hospital
Kettegård Allé 30
DK-2650 Hvidovre
Denmark
+45 38622166
kirsten.noergaard@regionh.dk

John Bagterp Jørgensen
Technical University of Denmark
Asmussens Allé, Building 303B
DK-2800 Kgs. Lyngby
Denmark
+45 45253088
jbjo@dtu.dk

Corresponding Author: Sabrina Lyngbye Wendt, Zealand Pharma A/S, Smedeland 36, DK-2600 Glostrup, Denmark; slw@zealandpharma.com

Abbreviations: (AP) artificial pancreas, (BMI) body mass index, (BW) body weight, (CI) confidence interval, (EGP) endogenous glucose production, (FDA) Food and Drug Administration, (HbA1c) glycated hemoglobin A1c, (MAP) maximum a posteriori, (ML) maximum likelihood, (ODE) ordinary differential equation, (PD) pharmacodynamics, (PK) pharmacokinetics, (SD) standard deviation, (SC) subcutaneous

Keywords: cross-validation, glucagon, glucoregulatory model, parameter estimation, simulation model, type 1 diabetes

3 figures (7 supplementary), 5 tables (10 supplementary)

Abstract

Background: Currently, no consensus exists on a model describing endogenous glucose production (EGP) as a function of glucagon concentrations. Reliable simulations to determine the glucagon dose preventing or treating hypoglycemia or to tune a dual-hormone artificial pancreas control algorithm need a validated glucoregulatory model including the effect of glucagon.

Methods: Eight type 1 diabetes (T1D) patients each received a subcutaneous (SC) bolus of insulin on four study days to induce mild hypoglycemia followed by a SC bolus of saline or 100, 200 or 300 µg of glucagon. Blood samples were analyzed for concentrations of glucagon, insulin and glucose. We fitted pharmacokinetic (PK) models to insulin and glucagon data using maximum likelihood and maximum a posteriori estimation methods. Similarly, we fitted a pharmacodynamic (PD) model to glucose data. The PD model included multiplicative effects of insulin and glucagon on EGP. Bias and precision of PD model test-fits were assessed by mean predictive error (MPE) and mean absolute predictive error (MAPE).

Results: Assuming constant variables in a subject across non-outlier visits and using thresholds of ±15% MPE and 20% MAPE, we accepted at least one and at most three PD model test-fits in each of the seven subjects. Thus, we successfully validated the PD model by leave-one-out cross-validation in seven out of eight T1D patients.

Conclusions: The PD model accurately simulates glucose excursions based on plasma insulin and glucagon concentrations. The reported PK/PD model including equations and fitted parameters allows for *in silico* experiments that may help improve diabetes treatment involving glucagon for prevention of hypoglycemia.

Introduction

The treatment goal for patients with type 1 diabetes is near-normalization of plasma glucose levels. Few patients achieve this even with intensive insulin treatment [1]. New approaches with automatic glucose controlled insulin and glucagon delivery, known as a dual-hormone artificial pancreas (AP), may offer a solution to improve glycemic control [2-6]. To design and tune control algorithms for AP devices prior to *in vivo* tests, a validated simulation model capturing the dynamics between glucose, insulin and glucagon is needed to perform helpful *in silico* experiments [7-9].

Glucagon primarily affects hepatic glucose production by increasing glycogenolysis, while the rate of gluconeogenesis seems less affected by changes in both insulin and glucagon concentrations [10]. Currently marketed glucagon is approved as a 1 mg rescue-treatment for severe hypoglycemia, although the interest in mini-dose glucagon is increasing [11, 12]. Recent studies proved that the glycemic response to low-dose glucagon is dependent on ambient insulin levels [13], but neither on plasma glucose level [14, 15] nor on prior glucagon dosing [16]. At high circulating insulin concentrations (50-60 mIU/l), the endogenous glucose production (EGP) is completely inhibited [17], and at insulin levels exceeding ~40 mIU/l the EGP cannot be stimulated by glucagon [13].

The ability of insulin to suppress the glycogenolytic response to glucagon at high insulin concentration is not reflected in previously published models of glucose-glucagon dynamics [18-20]. A comparative study found that a multiplicative relationship was needed to describe insulin's inhibitory effect and glucagon's stimulating effect on glycogenolysis with insulin overriding the effect of glucagon at high concentrations of both hormones [21]. Recently, we extended the multiplicative model by incorporating the interaction between insulin and glucagon on glycogenolysis [13, 22]. The model extension was developed using pre-clinical data from dogs and was fitted to clinical

human data in previous studies [23, 24]. In this paper, we aim to validate the multiplicative glucose-insulin-glucagon model for simulation studies in humans using data from eight patients with type 1 diabetes.

Methods

Data Collection

Clinical data originated from a glucagon dose-finding study in eight well-controlled patients with type 1 diabetes (5 females, age range: 19-64 years, BMI range: 20.0-25.4 kg/m^2, HbA1c range: 6.1-7.4 %), who were insulin pump-treated and had no endogenous production of insulin [25]. Table S1 summarizes the patient characteristics. In brief, the patients completed four similar study days in random order. On each study day, patients arrived at the research facility in the morning in a fasting state. A subcutaneous (SC) insulin bolus (NovoRapid®, Novo Nordisk A/S, Bagsværd, Denmark) was administered via the patient's insulin pump, aiming to lower plasma glucose to 54 mg/dl if no interventions were made. The insulin bolus was calculated based on each patient's individual sensitivity factor, which was determined prior to the first study visit using a standard procedure [26]. When plasma glucose reached ≤70 mg/dl, a single SC bolus of either 100 µg (visit B), 200 µg (visit C), 300 µg (visit D) glucagon (GlucaGen®, Novo Nordisk A/S, Bagsværd, Denmark), or saline (visit A) was administered, see Figure 1. Blood was sampled and analyzed for plasma glucose (YSI 2300 STAT Plus, Yellow Springs Instrument, Ohio), plasma glucagon [27] and serum insulin aspart (Mercodia AB, Uppsala, Sweden). The insulin pump continuously infused insulin as a basal rate during the study days. The insulin infusion rate was adjusted before the first study day, to keep near constant blood glucose values in the fasting and resting condition. The individual insulin infusion basal rates were similar between study visits.

Models

When applying a pharmacokinetic (PK) model, we assume that all increases in insulin and glucagon concentrations are due to exogenously dosed drugs so that endogenous production is constant or negligible.

Insulin Pharmacokinetic Model

Previous studies showed that a simple two-state model with identical time constants for absorption and elimination could be used to describe the PK of insulin aspart after SC dosing [28].

$$\frac{\mathrm{d}X_1(t)}{\mathrm{dt}} = u_I(t) - \frac{X_1(t)}{t_{max}}$$

$$\frac{\mathrm{d}X_2(t)}{\mathrm{dt}} = \frac{X_1(t)}{t_{max}} - \frac{X_2(t)}{t_{max}}$$

$$I(t) = \frac{1}{t_{max}} \frac{X_2(t)}{W \cdot Cl_{F,I}} 10^6 + I_b$$

Table 1 lists the interpretations of the insulin PK model parameters and their units. The insulin concentration in serum is the sum of external rapid acting insulin dosage and basal infusion. The model assumes steady state insulin concentration, I_b, maintained by the basal infusion when no exogenous rapid acting insulin is dosed.

Glucagon Pharmacokinetic Model

A two-state model with different absorption and elimination rate constants can describe glucagon PK after SC dosing [23].

$$\frac{\mathrm{d}Z_1(t)}{\mathrm{dt}} = u_C(t) - k_1 Z_1(t)$$

$$\frac{\mathrm{d}Z_2(t)}{\mathrm{dt}} = k_1 Z_1(t) - k_2 Z_2(t)$$

$$C(t) = \frac{k_2 Z_2(t)}{W \cdot Cl_{F,C}} + C_b$$

Table 1 lists the interpretations of the glucagon PK model parameters and their units. The glucagon concentration in plasma is the sum of constant endogenous glucagon, C_b, and external glucagon dosage. The model does not include an endogenous response to hypoglycemia.

Glucose Pharmacodynamic Model

The glucose PD model was originally derived by Hovorka *et al.* [29, 30] and further extended by Wendt *et al.* [23].

$$\frac{\mathrm{d}Q_1(t)}{\mathrm{dt}} = -F_{01} - F_R - S_T x_1(t) Q_1(t) + k_{12} Q_2(t) + G_{GG}(t) + G_{GNG}$$

$$\frac{\mathrm{d}Q_2(t)}{\mathrm{dt}} = S_T x_1(t) Q_1(t) - [k_{12} + S_D x_2(t)] Q_2(t)$$

$$G_{GG}(t) = \frac{1 - S_E x_3(t)}{1 - S_E I_b} \left((E_{max} - G_{GNG}) \frac{C(t)}{C_{E50} + C(t)} \right)$$

$$G(t) = \frac{Q_1(t)}{V}$$

$$\frac{\mathrm{d}x_1(t)}{\mathrm{dt}} = k_{a1}[I(t) - x_1(t)]$$

$$\frac{\mathrm{d}x_2(t)}{\mathrm{dt}} = k_{a2}[I(t) - x_2(t)]$$

$$\frac{\mathrm{d}x_3(t)}{\mathrm{dt}} = k_{a3}[I(t) - x_3(t)]$$

Table 1 lists the interpretations of the glucose PD model parameters and their units. The endogenous glucose production is the sum of glycogenolysis, G_{GG}, and gluconeogenesis, G_{GNG}. The gluconeogenesis is fixed at 6 µmol/kg/minute [10]. F_{01} is constant when plasma glucose concentration exceeds 81 mg/dl [30]. The renal glucose clearance is zero

when plasma glucose concentrations do not exceed 162 mg/dl [30]. The glucose volume of distribution is fixed at 160 ml/kg [29].

Model Fitting

All model fitting was executed in R version 3.1.0 Spring Dance using the additional packages CTSM-R and numDeriv [31]. Additional data handling was carried out using Microsoft Excel 2013. Unless stated otherwise, the results are reported as means with 95% Wald confidence intervals (CI) derived from the inverse Hessian, which provides the curvature of the log-likelihood function [32].

We fitted the insulin PK model using ordinary differential equations (ODEs) and estimated the log-normally distributed observation noise variance using maximum likelihood (ML) [33]. Due to missing insulin data around the expected time of maximum insulin concentration both t_{max} and $Cl_{F,I}$ were estimated using maximum a posteriori (MAP) while I_b was estimated using ML. Prior distributions of t_{max} and $Cl_{F,I}$ were reported in [28] and further information regarding t_{max} was extracted from the product monograph on insulin aspart [34]. Table S2 lists the prior parameter distributions. No prior correlation between t_{max} and $Cl_{F,I}$ was assumed.

Insulin PK parameters were optimized on a subject basis to datasets from all four visits (8 parameter sets reported). Despite SC infusion rates of short acting insulin (i.e. the basal rates) were similar per subject for all study visits, the baseline insulin concentration varied as evident from the raw data plotted in Figures S1-S7. Therefore, the parameter describing the steady state insulin level was estimated separately for each visit. Using the subject specific optimized parameters, the insulin PK was simulated every minute and used as input to the PD model.

We fitted the glucagon PK model for visits B, C, and D using ordinary differential equations (ODEs) and estimated the log-normally distributed observation noise variance using ML. Plasma glucagon was sampled adequately to perform ML estimation of all parameters in the glucagon PK model. There was some uncertainty regarding the exact dosing time of the glucagon bolus, which was given after the blood sampling at time zero but before the next blood sampling five minutes after. Due to this uncertainty, we estimated the dosing time by choosing the discrete dosing time within the five-minute interval yielding the fit with the highest likelihood value and kept this updated dosing time throughout the data fitting and handling.

As the absolute elimination rate of glucagon is limited by the absorption rate, glucagon exerts flip-flop kinetics [35]. To avoid the flip-flop phenomenon and to reduce the population variation in the two time constants, k_2 was parameterized such that it was greater than k_1 in all datasets.

The glucagon PK parameters were estimated to the datasets from visits with glucagon dosing (24 parameter sets, data not shown) and the PK simulated every minute to be used as input when fitting the PD model. On a subject basis, the glucagon PK parameters were optimized to datasets from all three glucagon visits (8 parameter sets reported). Due to the limited amount of data, we assumed the parameters did not differ between the visits.

The data following administration of saline (visit A) were not fitted to the glucagon PK model but described using linear interpolation between measurements. These interpolated data were used as inputs to the PD model.

The PD model was fitted using ordinary differential equations (ODEs) and the log-normally distributed observation noise variance estimated using ML. The remaining parameters (E_{max}, C_{E50}, F_{01}, k_{12}, k_{a1}, k_{a2}, k_{a3}, S_D, S_E, S_T) were estimated using MAP with

priors inspired by literature [22, 29]. We used priors for the time constants rather than fixing the four parameters [30]. The time constants and the insulin sensitivities were log-transformed during the parameter estimation. Table S2 lists the prior PD model parameter distributions. The PD model parameters have units yielding a glucose output measured in mmol/l, but the output is converted and graphically displayed with units of mg/dl. We assumed no prior correlation between parameters. As previously mentioned, glucose volume of distribution and gluconeogenesis were both fixed based on literature [10, 29]. I_b was fixed for each subject based on their average steady state insulin concentration. The final PD model parameters were obtained by optimizing the fit to all non-outlier visits by each subject (8 parameter sets reported).

Pharmacodynamic Model Validation

To quantify the simulation accuracy of the model on datasets not used for parameter optimization, the bias was calculated by the mean prediction error (MPE) and the precision calculated by the mean absolute prediction error (MAPE). MPE and MAPE were calculated as percentages [36].

$$MPE = \frac{1}{N}\sum_{j=1}^{N}\left[\left(\frac{pred_j - obs_j}{obs_j}\right)\times 100\right]$$

$$MAPE = \frac{1}{N}\sum_{j=1}^{N}\left[\left(\frac{\left|pred_j - obs_j\right|}{obs_j}\right)\times 100\right]$$

$pred_j$ and obs_j are the jth predicted and observed value, respectively of a total of N observations. If the MPE is less than ±15% and the MAPE is less than 20%, we regard the model fit as accurate, precise and suitable for simulations. Cut-off limits were based on categorizing some fits in “good”, “medium” and “bad” prior to knowledge of those fits’ MPE and MAPE values by two independent raters. The limits were chosen so that all

fits categorized as “good” by both raters would be accepted and all fits categorized as “bad” by both raters would not meet the acceptance criteria.

The PD model validation was carried out as a 4-fold leave-one-out cross-validation leaving all data from one visit out per fold. As each subject participated in four visits, each subject had four *training* datasets comprised of data from three visits and four corresponding *test* datasets with data from one visit:

- *Training*: B-C-D, *Test*: A
- *Training*: A-C-D, *Test*: B
- *Training*: A-B-D, *Test*: C
- *Training*: A-B-C, *Test*: D

Thus, all four visits were used for testing once without being used for optimization during that fold. If the MAPE of a test-fit exceeded 50 %, the test visit was considered an outlier and removed from further analysis. After removal of the outlier dataset another round of leave-one-out was performed on the remaining three datasets. To validate the PD model in a subject, we required that at least one PD model test-fit of a dataset from a glucagon visit (B, C or D) was accepted.

Results

Table 2 lists the estimated insulin PK model parameters. The fasting steady state insulin concentration had day-to-day variation within patients of up to 6 mU/l and ranged from 3.0 mU/l to 22.6 mU/l between subjects. The mean of all steady state insulin concentrations was 9.7 mU/l. The time to maximum concentration ranged from 40.8 to 68.5 minutes and the apparent clearance ranged 14.8-26.8 ml/kg/minute.

Table 3 lists the estimated glucagon PK model parameters and the calculated time to maximum concentration. The fasting steady state glucagon concentrations were similar in the range 7.6-11.6 pg/ml for all patients except patient 8 who had a concentration of 19.0 pg/ml. The absorption and elimination time constants ranged from 0.022-0.058 $minute^{-1}$ and 0.058-0.28 $minute^{-1}$, yielding a calculated time to maximum concentration of 7.5-19.1 minutes. The apparent clearance ranged from 91 to 200 ml/kg/minute.

Table 4 provides an overview of the leave-one-out cross-validation procedure of the PD model. The MPE and MAPE for the test-fits are listed together with a dichotomous decision of acceptance or not using the criteria outlined in section "Pharmacodynamic Model Validation". Based on the MAPE during leave-one-out, we excluded four outlier datasets from further analysis and these four patients had a second round of leave-one-out including the remaining three datasets. Overall, the test-fit was accepted two to three times out of three in three patients, and one to two times out of four in four patients. In patient 8 we did not accept any of the test-fits even after removal of an outlier dataset. Figure 2 presents examples of PD model test-fits and corresponding MPE and MAPE values of the test-fits both passing and violating the acceptance criteria. In summary, the PD model successfully predicted unseen glucose data at least once in seven patients and therefore we regard the PD model as validated and suitable for simulation studies of these seven type 1 diabetes patients.

Table 5 lists the PD model parameters optimized to all non-outlier visits in each patient with mean parameter values and 95% CI. The parameter describing the maximum EGP at steady state insulin concentration, E_{max}, ranged 56-84 µmol/kg/minute. The glucagon concentration at which the effect is half maximum, C_{E50}, ranged 141-436 pg/ml. Extrapolated to zero insulin and at basal glucagon concentration, the EGP ranged 7-13.3 µmol/kg/minute. According to the inverse of the parameter describing the insulin

sensitivity to EGP, S_E, the calculated insulin concentration at which the effect of glucagon shuts off ranged 22-71 mU/l. Figures 3 and S1-S7 provide simulations of patient optimized PD model fits and data.

Discussion

We fitted simple PK models of serum insulin and plasma glucagon after SC bolus administrations of the hormones. The simulated concentrations of insulin and glucagon were used as inputs to the PD model. We sought to validate the PD model for simulations in eight type 1 diabetes patients and succeeded in seven. Finally, we estimated the patient's individual PD model parameters.

The fitted insulin PK model assumes that all changes in serum insulin concentration are due to SC insulin dosing. This is a valid assumption as no patients had measureable endogenous insulin secretion after glucagon stimulation [25]. Patients' insulin levels are at steady state when no insulin bolus is administered.

The clinical study focused on generating data describing the effect of glucagon on glucose, and therefore only few data points describing the insulin PK were obtained. The insulin PK data were sampled very sparsely around the expected time of maximum concentration. The missing data did not allow for ML estimation of the insulin PK model. However, using literature informed prior distributions of both t_{max} and $Cl_{F,I}$ and optimizing for all four visits simultaneously we obtained reasonable fits by MAP estimation [28, 34].

As the insulin PK model was fitted to in-hospital sedentary patients, its application in patients with type 1 diabetes outside the hospital setting may be limited due to numerous factors affecting insulin absorption rate, sensitivity and bioavailability. Such factors could be accounted for by introducing time-variant model parameters, which was beyond the

scope of this work [9, 37, 38]. Especially, differences in insulin absorption could explain the observed intra-patient variation in steady state insulin concentration despite equal basal rates at all four visits.

Patients with type 1 diabetes have a blunted glucagon response to hypoglycemia compared to healthy subjects [39]. The fitted glucagon PK model assumes that all changes in plasma glucagon concentration are due to SC dosing and that the endogenous production is constant or negligible. To verify this assumption, we determined the size of the endogenous glucagon response to hypoglycemia during the saline day and compared it to simulations of glucagon PK in each of the eight subjects (data not shown). We found that exogenous glucagon doses of 1-10 µg would equal the plasma glucagon increase to hypoglycemia. Since the endogenous glucagon response to hypoglycemia was at most one tenth of the administered dose during the glucagon days, this confirmed that the endogenous response during these days was negligible compared to the exogenous dosed glucagon. However, the endogenous response was not negligible during the saline day and therefore the glucagon PK model was not applicable to those datasets.

The glucagon PK fit was challenged by the short time to maximum concentration combined with the uncertainty of the exact dosing time of glucagon. This could potentially result in an error in time to maximum concentration of up to ±4 minutes. However, this possible deviation has minor impact on the PD model fit when the glucagon PK fit is used as an input. Despite the dosing time uncertainty, the calculated times to maximum concentration are within reasonable range of population averages reported in the literature [28, 40]. In the model by Haidar *et al.* [28], the glucagon absorption rate and elimination rate were identical which we only observed in patient 4. In the remaining seven patients, the elimination rate was significantly higher than the absorption rate. Moreover, having different absorption and elimination rate constants we

observed a higher clearance rate. Compared to Haidar *et al.*, we found lower basal concentration of glucagon, which could be attributed to differences in the assays for analysis of plasma glucagon concentration [26].

Despite using informed priors for all PD model parameters, some optimized parameters are very different from the population mean and vary considerably more than originally listed in Hovorka *et al.* [29]. However, the original reference is based on a population of only six subjects, which makes it unlikely that all true population variations were captured, and we believe, therefore, that our parameter estimates are still valid. Similarly, with a population of eight subjects, we did not fit a population model but focused on estimating parameters for each subject individually.

The limited human data on EGP response to glucagon are consistent with data from dogs [22]. As the human response to high glucagon concentrations has not been thoroughly investigated, the dog data provide best guesses of the human values. The maximum EGP due to glucagon and glucagon concentration at half-maximum effect at basal insulin average around 60 µmol/kg/minute and 300 pg/ml in dogs [22]. Our results match the reference values and therefore seem plausible.

We found that EGP at zero insulin and basal glucagon is somewhat lower than previous publications, which state 10-20 µmol/kg/minute [29] and ~30 µmol/kg/minute [22]. This might be due to the fixation of gluconeogenesis at 6 µmol/kg/minute [10], which is increased in subjects with poorly controlled type 1 diabetes compared to the present well-controlled patients or healthy subjects [25, 41]. Assuming the proposed model of EGP is correct, the insulin concentration at which the glycogenolysis, hence the effect of glucagon, shuts off is reasonable compared to the limited publications showing glycogenolysis at various insulin concentrations [22, 42]. Rizza *et al*. found that the glucose production was suppressed by insulin beyond approximately 60 mU/l [17]. El

Youssef *et al.* found that at serum insulin concentrations beyond 40 mU/l glucagon concentrations below 450 pg/ml did not stimulate EGP [13]. Further clinical studies are needed to investigate whether high insulin concentrations completely suppress the effect of glucagon or whether the maximum EGP is still attainable though at higher glucagon concentrations.

A major limitation to some of the previously published models describing the effect of glucagon on glucose production is lack of validation [18, 21]. We were able to mimic never-before-seen glucose data at least once and at most three times in seven of the eight subjects using the presented glucose PD model. We did not expect to accept the test-fit of all non-outlier datasets in each subject as the visits often described complimentary dynamics of the glucose-insulin-glucagon relationship; for instance the placebo day had very limited information on how different glucagon concentrations affects EGP as glucagon levels were changing very little. On the contrary, the placebo datasets were rich in information about the effects of insulin on plasma glucose. Some glucagon datasets had few observations of the effects of insulin on EGP as the plasma glucose some days reached the bolus threshold of 70 mg/dl quickly e.g. in subject 2 and 7 shown in Figure S2 and Figure 3, respectively. As an example, this difference in data sampling can explain why it was not possible to validate the model using subject 2's visit B as the test dataset. For this particular patient, the placebo visit was stopped early and therefore does not contain much information about the insulin dynamics. Moreover, the insulin only phase of visit B lasted nearly five hours and only two hours during visit C and D. Leaving visit B out of the training dataset does not provide the model with enough information to predict the insulin dynamics present in visit B. We noted that in most cases when the test-fit was not accepted there was a monotone bias in the residuals yielding almost equal values of absolute MPE and MAPE, see Table 4. This bias indicates that the test-fit

would either over- or undershoot compared to data and thus both insulin and glucagon dynamics of the test dataset were not well described by the training datasets. Analyzing the PD model parameters during leave-one-out in Tables S3-S10, we observed that when a test-fit could not be accepted, usually one or more parameters were outside the CI obtained when fitting to all non-outlier data. Therefore, failing to accept the test-fit during a fold is not necessarily a sign of an incorrect model structure. Rather it could emphasize that the test dataset contains unique information about the dynamics, which are not present in any of the training datasets [43]. However, in four patients one dataset was so different from the other three datasets that it had to be excluded from the final PD model estimation as it would otherwise affect the parameters and yield bad fits for all four study days.

Simulation models are rarely validated on unseen data. The only glucose model including glucagon that is currently validated and FDA approved has undisclosed parameter values and can only be accessed by payment [19, 44]. We believe that this paper is a step towards more openly sharing simulation models that will allow more research groups to test dual-hormone dosing strategies and control algorithms for managing diabetes before carrying out expensive simulations or clinical trials.

Conclusion

We have successfully validated a model describing the glucose-insulin-glucagon dynamics in seven type 1 diabetes subjects using leave-one-out cross-validation. We have reported model parameter sets with uncertainties for each subject, which could be used for *in silico* experiments. Simulations could also aid in optimizing treatment for type 1 diabetes patients such as glucagon dosing strategies for preventing hypoglycemia and tuning control strategies for an AP.

Funding Sources

The authors disclosed receipt of the following financial support for the research, authorship and/or publication of this article: This study was supported by Zealand Pharma A/S and the Innovation Fund Denmark. Further, the study was supported by the Danish Diabetes Academy funded by the Novo Nordisk Foundation.

Acknowledgements

None.

Disclosures

SLW is a full time employee of Zealand Pharma. SS serves on the continuous glucose monitoring advisory board of Roche Diabetes Care and as a consultant to Unomedical. CBK is a full time employee of Zealand Pharma and owns shares in Zealand Pharma. JJH has consulted for Merck Sharp & Dome, Novo Nordisk and Roche. SM has served as a consultant or adviser to Amgen, Astra-Zeneca, Boehringer-Ingelheim, Bristol-Myers Squibb, Eli Lilly, Intarcia Therapeutics, Johnson & Johnson, Merck Sharp & Dohme, Novo Nordisk, Novartis Pharma and Sanofi, has received a research grant from Novo Nordisk and has received fees for speaking from Astra-Zeneca, Bristol-Myers Squibb, Eli Lilly, Merck, Sharp & Dohme, Novo Nordisk, Novartis Pharma and Sanofi. KN serves as adviser to Medtronic, Abbott and Novo Nordisk, owns shares in Novo Nordisk, has received research grants from Novo Nordisk and has received fees for speaking from Medtronic, Roche, Rubin Medical, Sanofi, Novo Nordisk, Bayer and Zealand Pharma. JBJ has served as a consultant for Novo Nordisk.

References

[1] Diabetes Control and Complications Trial Research Group. The effect of intensive treatment of diabetes on the development and progression of long-term complications in insulin-dependent diabetes mellitus. N Engl J Med. 1993; 329: 977-986.

[2] Bátora V, Tárník M, Murgaš J, Schmidt S, Nørgaard K, Poulsen NK *et al.* The contribution of glucagon in an artificial pancreas for people with type 1 diabetes. Proceedings of the 2015 American Control Conference; 2015 Jul 1-3; Chicago, Illinois. IEEE; 2015. p. 5097-5102.

[3] Blauw H, van Bon AC, Koops R, DeVries JH. Performance and safety of an integrated bihormonal artificial pancreas for fully automated glucose control at home. Diabetes Obes Metab. 2016; 18(7): 671-677.

[4] Haidar A, Rabasa-Lhoret R, Legault L, Lovblom LE, Rakheja R, Messier V *et al*. Single- and dual-hormone artificial pancreas for overnight glucose control in type 1 diabetes. J Clin Endocrinol Metab. 2016; 101(1): 214-223.

[5] Jacobs PG, El Youssef J, Reddy R, Resalat N, Branigan D, Condon J *et al.* Randomized trial of a dual-hormone artificial pancreas with dosing adjustment during exercise compared with no adjustment and sensor-augmented pump therapy. Diabetes Obes Metab. 2016; Epub 2016 Aug 15.

[6] Russell SJ, Hillard MA, Balliro C, Magyar KL, Selagamsetty R, Sinha M *et al.* Day and night glycaemic control with a bionic pancreas versus conventional insulin pump therapy in preadolescent children with type 1 diabetes: a randomised crossover trial. Lancet Diabetes Endocrinol. 2016; 4: 233-243.

[7] Haidar A. The artificial pancreas: How closed-loop control is revolutionizing diabetes. IEEE Control Syst Mag. 2016; 36(5): 28-47.

[8] Kirchsteiger H, Jørgensen JB, Renard E, del Re L, editors. Prediction methods for blood glucose concentration: Design, use and evaluation. 1st ed. Springer; 2016.

[9] Mansell EJ, Docherty PD, Chase JG. Shedding light on grey noise in diabetes modelling. Biomed Signal Process Control. 2017; 31: 16-30.

[10] Nuttall FQ, Ngo A, Gannon MC. Regulation of hepatic glucose production and the role of gluconeogenesis in humans: is the rate of gluconeogenesis constant? Diabetes Metab Res Rev. 2008; 24: 438-458.

[11] Chung ST, Haymond MW. Minimizing morbidity of hypoglycemia in diabetes: A review of mini-dose glucagon. J Diabetes Sci Technol. 2015; 9(1): 44-51.

[12] Taleb N, Haidar A, Messier V, Gingras V, Legault L, Rabasa-Lhoret R. Glucagon in the artificial pancreas systems; potential benefits and safety profile of future chronic use. Diabetes Obes Metab. 2016; Epub 2016 Sep 15.

[13] El Youssef J, Castle JR, Bakhtiani PA, Haidar A, Branigan DL, Breen M *et al*. Quantification of the glycemic response to microdoses of subcutaneous glucagon at varying insulin levels. Diabetes Care. 2014; 37(11): 3054-3060.

[14] Blauw H, Wendl I, DeVries JH, Heise T, Jax T. Pharmacokinetics and pharmacodynamics of various glucagon dosages at different blood glucose levels. Diabetes Obes Metab. 2016; 18(1): 34-39.

[15] Hinshaw L, Mallad A, Man CD, Basu R, Cobelli C, Carter RE *et al.* Glucagon sensitivity and clearance in type 1 diabetes: insights from in vivo and in silico experiments. Am J Physiol Endocrinol Metab. 2015; 309(5): E474-E486.

[16] Castle JR, Youssef JE, Bakhtiani PA, Cai Y, Stobbe JM, Branigan D, *et al*. Effect of repeated glucagon doses on hepatic glycogen in type 1 diabetes: Implications for a bihormonal closed-loop system. Diabetes Care. 2015; 38(11): 2115-2119.

[17] Rizza RA, Mandarino LJ, Gerich JE. Dose-response characteristics for effects of insulin on production and utilization of glucose in man. Am J Physiol Endocrinol Metab. 1981; 240: E630-E639.

[18] Herrero P, Georgiou P, Oliver N, Reddy M, Johnston D, Toumazou C. A composite model of glucagon-glucose dynamics for *in silico* testing of bihormonal glucose controllers. J Diabetes Sci Technol. 2013; 7(4): 941-951.

[19] Man CD, Micheletto F, Lv D, Breton M, Kovatchev B, Cobelli C. The UVA/PADOVA type 1 diabetes simulator: New features. J Diabetes Sci Technol. 2014; 8(1): 26-34.

[20] Peng JZ, Denney WS, Musser BJ, Liu R, Tsai K, Fang L *et al.* A semi-mechanistic model for the effects of a novel glucagon receptor antagonist on glucagon and the interaction between glucose, glucagon, and insulin applied to adaptive phase II design. AAPS J. 2014; 16(6): 1259-1270.

[21] Emami A, El Youssef J, Rabasa-Lhoret R, Pineau J, Castle JR, Haidar A. Modelling glucagon action in patients with type 1 diabetes. IEEE J Biomed Health Inform. 2016; Epub 2016 Jul 20.

[22] Cherrington AD. Control of glucose production in vivo by insulin and glucagon. Comprehensive physiology 2011, supplement 21: Handbook of physiology, the endocrine system, the endocrine pancreas and regulation of metabolism. 2001; 759-785.

[23] Wendt SL, Møller JK, Knudsen CB, Madsen H, Haidar A, Jørgensen JB. PK/PD modelling of glucose-insulin-glucagon dynamics in healthy dogs after a subcutaneous bolus administration of native glucagon or a novel glucagon analogue. Final report. Technical University of Denmark, DTU Compute, Kgs. Lyngby, Denmark. 2016. Report No.: 2016-2.

[24] Wendt SL, Møller JK, Haidar A, Knudsen CB, Madsen H, Jørgensen JB. Modelling of glucose-insulin-glucagon pharmacodynamics in man. IEEE EMBC 2016: Proceedings of the 38th Annual International Conference of the IEEE Engineering in Medicine and Biology Society; 2016 Aug 16-20; Orlando, Florida. IEEE; 2016.

[25] Ranjan A, Schmidt S, Madsbad S, Holst JJ, Nørgaard K. Effects of subcutaneous, low-dose glucagon on insulin-induced mild hypoglycaemia in patients with insulin pump treated type 1 diabetes. Diabetes Obes Metab. 2016; 18(4): 410-418.

[26] Walsh J, Roberts R. Pumping insulin: Everything you need for success on a smart insulin pump. 4th ed. Torrey Pines; 2006.

[27] Albrechtsen NJW, Hartmann B, Veedfald S, Windeløv JA, Plamboeck A, Bojsen-Møller KN *et al*. Hyperglucagonaemia analysed by glucagon sandwich ELISA: nonspecific interference or truly elevated levels? Diabetologia. 2014; 57(9): 1919-1926.

[28] Haidar A, Duval C, Legault L, Rabasa-Lhoret R. Pharmacokinetics of insulin aspart and glucagon in type 1 diabetes during closed-loop operation. J Diabetes Sci Technol. 2013; 7(6): 1507-1512.

[29] Hovorka R, Shojaee-Moradie F, Carroll PV, Chassin LJ, Gowrie IJ, Jackson NC *et al.* Partitioning glucose distribution/transport, disposal, and endogenous production during IVGTT. Am J Physiol Endocrinol Metab. 2002; 282: E992-E1007.

[30] Hovorka R, Canonico V, Chassin LJ, Haueter U, Massi-Benedetti M, Federici MO *et al.* Nonlinear model predictive control of glucose concentration in subjects with type 1 diabetes. Physiol Meas. 2004; 25: 905-920.

[31] Juhl R, Møller JK, Jørgensen JB, Madsen H. Modeling and prediction using stochastic differential equations. In Kirchsteiger H, Jørgensen JB, Renard E, del Re L, editors. Prediction methods for blood glucose concentration: Design, use and evaluation. Switzerland: Springer; 2016. p 183-209.

[32] Madsen H, Thyregod P. Introduction to general and generalized linear models. 1st ed. CRC Press; 2011.

[33] Kristensen NR, Madsen H, Jørgensen SB. Parameter estimation in stochastic grey-box models. Automatica. 2004; 40(2): 225-237.

[34] Novo Nordisk A/S. Product Monograph, schedule D, NovoRapid®, insulin aspart. [updated March 11, 2016; cited August 24, 2016]. Available from. http://www.novonordisk.ca/content/dam/Canada/AFFILIATE/www-novonordisk-ca/OurProducts/PDF/novorapid-product-monograph.pdf

[35] Gabrielsson J, Weiner D. Pharmacokinetic & pharmacodynamic data analysis: Concepts and applications. 4th ed. Apotekarsocieteten; 2006.

[36] Owen JS, Fiedler-Kelly J. Introduction to population pharmacokinetic/ pharmacodynamic analysis with nonlinear mixed effects models. 1st ed. Wiley; 2014.

[37] Hildebrandt P. Subcutaneous absorption of insulin in insulin-dependent diabetic patients. Influence of species, physico-chemical properties of insulin and physiological factors. Danish medical bulletin 1991; 38(4): 337-346.

[38] DeFronzo R, Simonson D, Ferrannini E. Hepatic and peripheral insulin resistance: A common feature of type 2 (non-insulin-dependent) and type 1 (insulin-dependent) diabetes mellitus. Diabetologia. 1982; 23(4): 313-319.

[39] Arbelaez AM, Xing D, Cryer PE, Kollman C, Beck RW, Sherr J *et al*. Blunted glucagon but not epinephrine responses to hypoglycemia occurs in youth with less than 1 yr duration of type 1 diabetes mellitus. Pediatr Diabetes. 2014; 15(2): 127-134.

[40] Novo Nordisk A/S. Product Monograph, GlucaGen®, glucagon. [updated June 1, 2016; cited October 6, 2016]. Available from http://www.paladin-labs.com/our_products/PM_GlucaGen_EN.pdf

[41] Kacerovsky M, Jones J, Schmid AI, Barosa C, Lettner A, Kacerovsky-Bielesz G *et al*. Postprandial and fasting hepatic glucose fluxes in long-standing type 1 diabetes. Diabetes. 2011; 60: 1752-1758.

[42] Adkins A, Basu R, Persson M, Dicke B, Shah P, Vella A *et al*. Higher insulin concentrations are required to suppress gluconeogenesis than glycogenolysis in nondiabetic humans. Diabetes. 2003; 52: 2213-2220.

[43] Kreutz C, Raue A, Kaschek D, Timmer J. Profile likelihood in systems biology. FEBS J. 2013; 208: 2564-2571.

[44] Kovatchev BP, Breton M, Man CD, Cobelli C. *In silico* preclinical trials: A proof of concept in closed-loop control of type 1 diabetes. J Diabetes Sci Technol. 2009; 3(1): 44-55.

Tables

Table 1: Interpretation of insulin PK (top rows), glucagon PK (middle rows) and glucose PD (bottom rows) model parameters and their units.

Parameter	**Unit**	**Interpretation**
$X_1(t)$	U	insulin mass due to exogenous dosing, in SC tissue
$X_2(t)$	U	insulin mass due to exogenous dosing, in serum
$u_I(t)$	U/minute	insulin dose
t_{max}	minutes	time from dose to maximum serum concentration
W	kg	body weight
$Cl_{F,I}$	ml/kg/minute	apparent insulin clearance
I_b	mU/l	steady state insulin concentration
$I(t)$	mU/l	insulin concentration in serum
$Z_1(t)$	pg	glucagon mass due to exogenous dosing, in SC tissue
$Z_2(t)$	pg	glucagon mass due to exogenous dosing, in plasma
$u_C(t)$	pg/minute	glucagon dose
k_1	$minute^{-1}$	absorption rate constant
k_2	$minute^{-1}$	elimination rate constant
$Cl_{F,C}$	ml/kg/minute	apparent glucagon clearance
C_b	pg/ml	steady state glucagon concentration
$C(t)$	pg/ml	glucagon concentration in plasma
$Q_1(t)$	µmol/kg	glucose mass per W in the accessible compartment
$Q_2(t)$	µmol/kg	glucose mass per W in the non-accessible compartment
$x_1(t)$	mU/l	remote effects of insulin on glucose transport
$x_2(t)$	mU/l	remote effects of insulin on glucose disposal

$x_3(t)$	mU/l	remote effects of insulin on glycogenolysis
$G(t)$	mmol/l	glucose concentration in plasma
$G_{GG}(t)$	µmol/kg/minute	glucose production due to glycogenolysis
G_{GNG}	µmol/kg/minute	glucose production due to gluconeogenesis
F_{01}	µmol/kg/minute	insulin independent glucose flux
F_R	µmol/kg/minute	renal glucose clearance
S_T	$minute^{-1}/(mU/l)$	insulin sensitivity of glucose transport
S_D	$minute^{-1}/(mU/l)$	insulin sensitivity of glucose disposal
S_E	l/mU	insulin sensitivity on glycogenolysis
k_{12}	$minute^{-1}$	transfer rate constant from the non-accessible to the accessible compartment
k_{a1}	$minute^{-1}$	insulin deactivation rate constant
k_{a2}	$minute^{-1}$	insulin deactivation rate constant
k_{a3}	$minute^{-1}$	insulin deactivation rate constant
E_{max}	µmol/kg/minute	maximum EGP at basal insulin concentration
C_{E50}	pg/ml	glucagon concentration yielding half of maximum EGP
V	ml/kg	glucose volume of distribution

Table 2: Summary of insulin PK model parameters for simulation with range of means and 95% CI or mean and 95% CI.

Patient	I_b **[mU/l]**	t_{max} **[min]**	$Cl_{F,I}$ **[ml/kg/min]**
1	6.6-7.8 (6.0-8.3)	57.6 (50.9-64.3)	18.9 (17.3-20.6)
2	10.0-11.2 (9.1-12.0)	57.3 (48.8-65.9)	18.5 (16.1-21.2)
3	10.3-13.4 (9.7-14.0)	40.8 (37.6-44.0)	14.8 (13.6-16.1)
4	7.8-9.4 (7.4-9.9)	67.9 (63.5-72.2)	17.4 (16.6-18.3)
5	5.2-8.2 (4.8-8.8)	48.5 (44.7-52.4)	17.3 (15.7-19.0)
6	3.0-8.5 (2.3-9.4)	46.5 (41.7-51.3)	24.6 (22.9-26.3)
7	16.8-22.6 (15.6-23.6)	68.5 (60.6-76.4)	23.7 (21.3-26.4)
8	4.7-9.1 (4.4-9.6)	55.4 (49.6-61.2)	26.8 (24.8-29.0)

Table 3: Summary of glucagon PK model parameters for simulation with mean and 95% CI.

Patient	C_b **[pg/ml]**	k_1 **[min^{-1}]**	k_2 **[min^{-1}]**	$Cl_{F,C}$ **[ml/kg/min]**	t_{max} **[min]**
1	10.7 (9.4-12.0)	0.042 (0.036-0.048)	0.14 (0.10-0.22)	94 (83-105)	12.2
2	7.6 (6.9-8.3)	0.056 (0.052-0.062)	0.26 (0.18-0.38)	106 (96-116)	7.5
3	7.6 (5.9-9.3)	0.022 (0.018-0.028)	0.10 (0.06-0.17)	114 (96-132)	19.1
4	10.9 (9.2-12.6)	0.058 (0.011-0.313)	0.058 (NA)	159 (133-184)	17.3
5	8.7 (7.7-9.8)	0.038 (0.032-0.044)	0.19 (0.13-0.29)	200 (176-223)	10.7
6	8.9 (7.8-10.0)	0.035 (0.031-0.040)	0.28 (0.19-0.41)	125 (111-138)	8.6
7	11.6 (10.1-13.0)	0.035 (0.030-0.041)	0.25 (0.16-0.39)	136 (120-152)	9.2
8	19.0 (16.1-22.0)	0.052 (0.037-0.072)	0.090 (0.04-0.26)	91 (78-105)	14.5

Table 4: PD model validation using leave-one-out cross-validation. Initially, data from three visits are used for training the model, i.e. optimizing model parameters, and data from the fourth visit is used for testing the model with the optimized parameters. *A test-fit with MPE or MAPE exceeding 50% is considered an outlier. The outlier dataset is removed and another round of leave-one-out cross-validation is performed on the remaining three visits.

Patient	Training visits	Test visit	MPE, %	MAPE, %	Accept? (Y/N)
1	BCD	A	-25.0	25.0	N
	ACD	B	-11.3	13.7	Y
	ABD	C	78.8	78.8	N*
	ABC	D	3.3	25.5	N
	BD	A	-10.3	11.1	Y
	AD	B	10.4	13.1	Y
	AB	D	4.0	21.3	N
2	BCD	A	29.1	29.8	N
	ACD	B	-18.2	18.7	N
	ABD	C	-6.3	7.5	Y
	ABC	D	6.3	10.0	Y
3	BCD	A	10.3	17.4	Y
	ACD	B	-2.3	8.6	Y
	ABD	C	23.4	24.6	N
	ABC	D	-20.1	20.1	N
4	BCD	A	-17.3	18.9	N
	ACD	B	-9.4	11.1	Y
	ABD	C	-23.6	23.7	N
	ABC	D	38.2	38.4	N
5	BCD	A	-13.4	13.4	Y
	ACD	B	-30.0	30.4	N
	ABD	C	-16.3	21.3	N
	ABC	D	74.6	74.6	N*
	BC	A	-1.7	4.5	Y

	AC	B	-9.8	14.1	Y
	AB	C	-7.5	17.4	Y
6	BCD	A	-23.5	24.2	N
	ACD	B	-4.5	12.0	Y
	ABD	C	59.0	59.0	N*
	ABC	D	-8.6	16.3	Y
	BD	A	-13.7	16.9	Y
	AD	B	16.7	17.5	N
	AB	D	4.7	15.8	Y
7	BCD	A	43.0	43.3	N
	ACD	B	-19.0	19.0	N
	ABD	C	-2.9	19.0	Y
	ABC	D	6.0	8.0	Y
8	BCD	A	-8.0	12.4	Y
	ACD	B	-32.9	33.0	N
	ABD	C	-14.5	24.2	N
	ABC	D	174.1	174.1	N*
	BC	A	-26.2	26.2	N
	AC	B	-24.6	24.6	N
	AB	C	42.5	42.5	N

Table 5: Summary of PD model parameters for simulation with mean and 95% CI.

ID	Data	C_{E50} [pg/ml]	E_{max} [µmol/kg/min]	F_{01} [µmol/kg/min]	k_{12}*10^{-4} [min^{-1}]	k_{a1}*10^{-4} [min^{-1}]	k_{a2}*10^{-4} [min^{-1}]	k_{a3}*10^{-4} [min^{-1}]	S_D*10^{-4} [min^{-1}/(mU/l)]	S_E*10^{-4} [(mU/l)$^{-1}$]	S_T*10^{-4} [min^{-1}/(mU/l)]
1	ABD	436 (355-517)	56.4 (51.1-61.8)	14.2 (12.9-15.5)	244 (181-330)	16 (7-35)	522 (221-1233)	215 (59-778)	1.5 (0.6-3.3)	155 (83-289)	23 (16-31)
2	ABCD	405 (339-471)	67.4 (59.3-75.5)	13.8 (12.8-14.7)	285 (223-363)	15 (7-35)	495 (236-1039)	231 (137-389)	1.2 (0.6-2.3)	334 (232-481)	19 (15-25)
3	ABCD	401 (327-475)	57.4 (49.8-65.0)	15.5 (14.2-16.8)	397 (277-568)	18 (8-42)	548 (268-1121)	327 (168-638)	1.4 (0.7-2.5)	237 (183-308)	25 (17-36)
4	ABCD	285 (226-344)	84.4 (73.9-94.8)	12.8 (11.3-14.4)	213 (157-289)	18 (9-36)	437 (183-1044)	68 (42-113)	2.0 (1.0-3.8)	415 (347-496)	18 (13-25)
5	ABC	339 (251-427)	65.4 (53.8-77.1)	12.0 (10.6-13.5)	281 (194-406)	15 (7-32)	517 (223-1201)	235 (95-586)	1.1 (0.4-2.6)	229 (127-415)	31 (20-47)
6	ABD	424 (333-515)	60.1 (46.3-74.0)	13.1 (11.7-14.5)	238 (172-330)	10 (4-22)	353 (102-1221)	74 (23-232)	2.6 (1.1-6.2)	404 (185-882)	21 (14-32)
7	ABCD	141 (96-187)	78.0 (68.9-87.1)	14.2 (12.2-16.1)	358 (252-509)	49 (23-105)	624 (319-1221)	178 (69-459)	4.4 (3.2-6.0)	140 (99-199)	21 (16-29)
8	ABC	307 (228-386)	75.3 (61.5-89.1)	13.4 (11.4-15.4)	289 (197-424)	37 (18-75)	518 (203-1324)	154 (68-348)	4.2 (2.8-6.5)	463 (377-569)	29 (20-42)

Figures

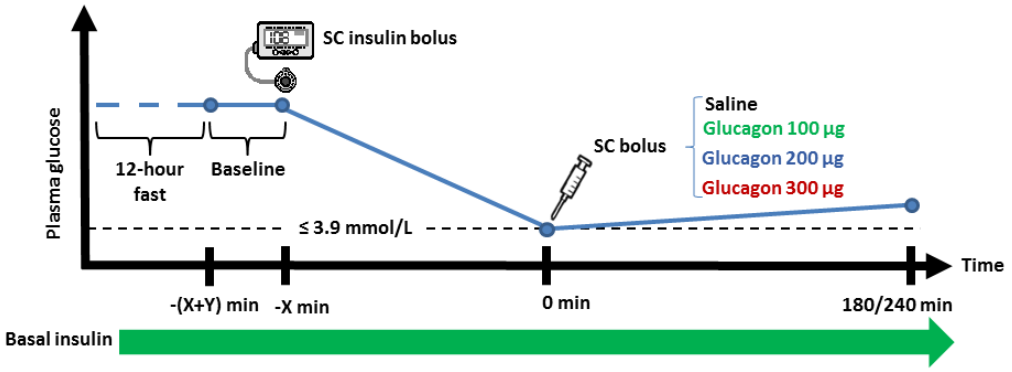

Figure 1: Schematic design of the study days. Baseline blood samples were taken at time –(X+Y). An insulin bolus was given after Y minutes. In a few cases, multiple insulin boluses had to be administered to lower the plasma glucose sufficiently. When the plasma glucose measured below 70 mg/dl, a saline or glucagon bolus was given depending on the study day. At 180 or 240 minutes after the saline/glucagon bolus the experiment was stopped. Basal insulin infusion continued throughout the experiment. From t=–x to t=0, plasma glucose was measured every 15-30 minutes, while plasma glucagon and serum insulin were measured every 60 minutes. Plasma glucose was measured every 5 minutes from t=0 to t=60, every 10 minutes from t=60-120 and then every 15 minutes. Plasma glucagon and serum insulin were measured every 5 minutes from t=0 to t=15, every 15 minutes from t=15 to t=60, every 30 minutes from t=60 to t=120, and then every 60 minutes.

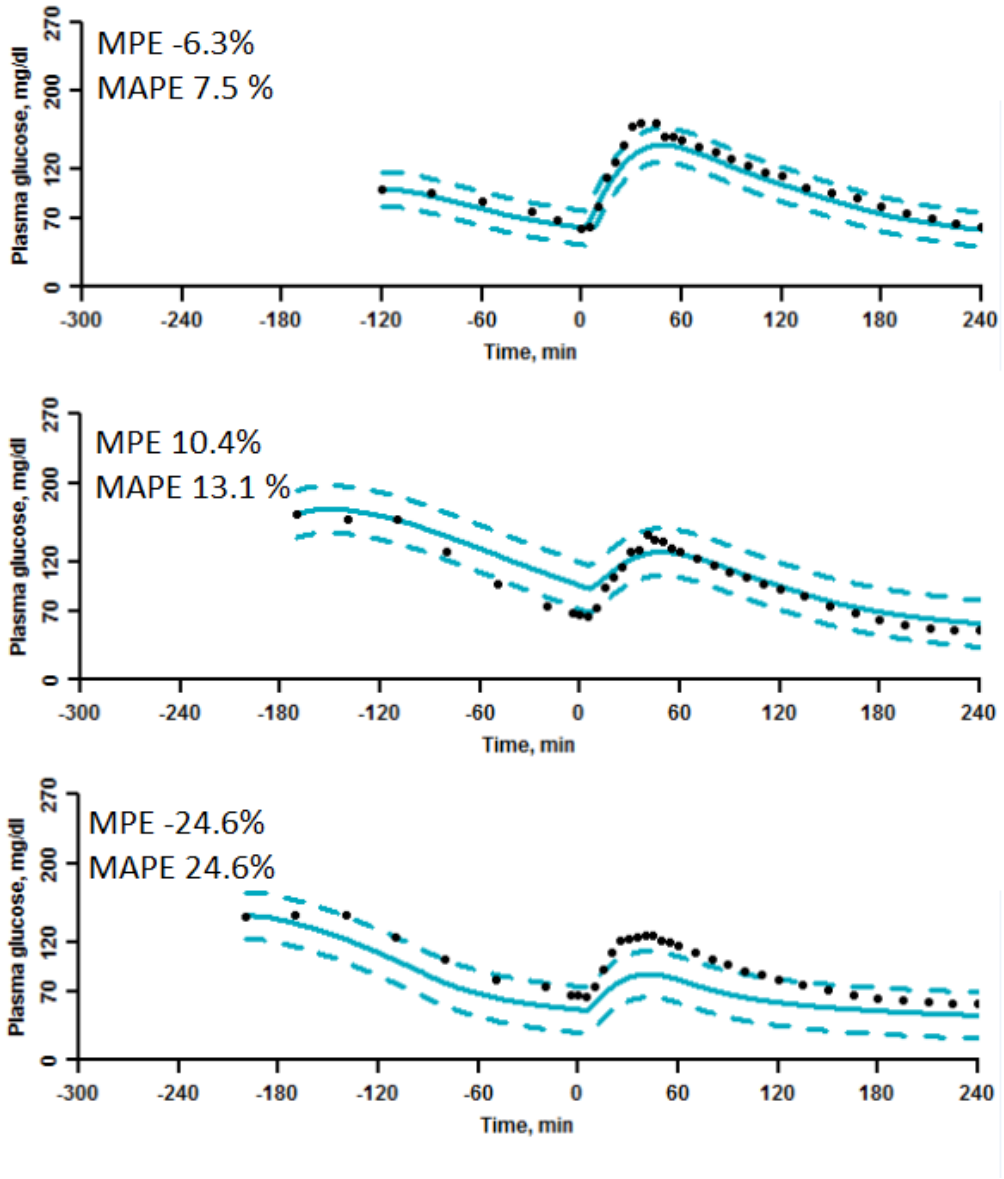

Figure 2: Examples of validation PD model fits with “good”, “medium” and “bad” MPE and MAPE. Top graph is test of patient 2’s visit C (accepted). Middle graph is test of patient 1’s visit B (accepted). Bottom graph is test of patient 8’s visit B (not accepted).

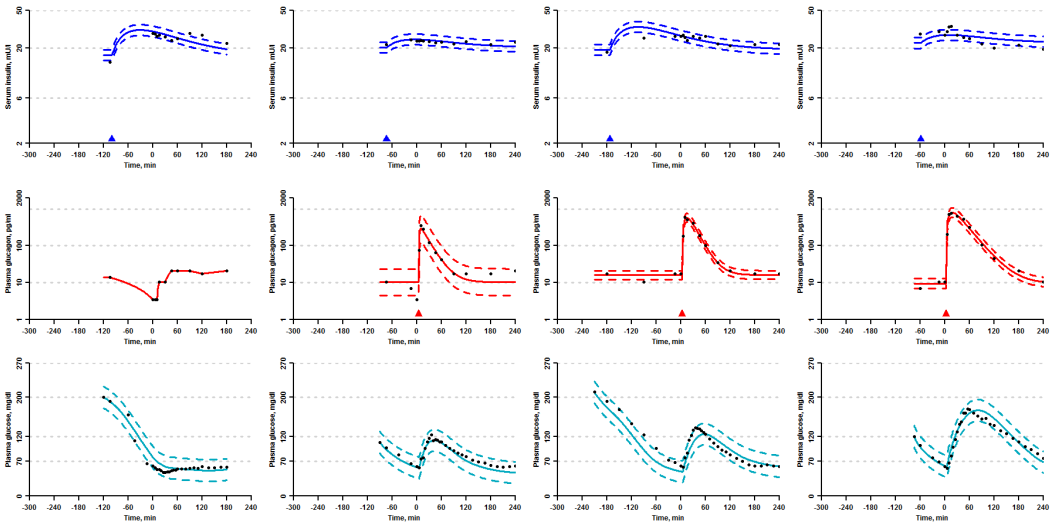

Figure 3: Data from all patient 7's visits (left to right: visit A to D) with insulin PK model fits (top row, logarithmic y-axes) and glucagon linear interpolation or PK model fits (middle row, logarithmic y-axes) both used as inputs to the glucose PD model for simulation built with data from all four visits (bottom row). The triangles indicate dose time of the insulin and glucagon boluses, respectively.